

STRUCTURAL, MECHANICAL AND CYTOTOXICITY CHARACTERIZATION OF AS-CAST BIODEGRADABLE Zn-xMg ($x = 0.8-8.3$ %) ALLOYS

STRUKTURNE, MEHANSKE IN CITOTOKSIČNE LASTNOSTI BIORAZGRADLJIVE Zn-xMg ($x = 0,8-8,3$ %) ZLITINE V LITEM STANJU

Jiří Kubásek¹, Iva Pospíšilová¹, Dalibor Vojtěch¹, Eva Jablonská², Tomáš Ruml²

¹Department of Metals and Corrosion Engineering, Institute of Chemical Technology, Prague, Technická 5, 166 28 Prague 6, Czech Republic

²Department of Microbiology, Institute of Chemical Technology, Prague, Technická 5, 166 28 Prague 6, Czech Republic
kubasek.jiri@gmail.com

Prejem rokopisa – received: 2013-04-05; sprejem za objavo – accepted for publication: 2013-11-04

In the present work, the structural, tensile, compressive and bending mechanical properties as well as the cytotoxicity of the Zn-Mg biodegradable alloys containing mass fractions from 0 % up to 8.3 % Mg were studied. It was found that the maximum tensile and compressive strengths of 170 MPa and 320 MPa, respectively, were obtained for the Zn-0.8Mg alloy. This alloy also showed the highest tensile elongation of 2 %. Mechanical properties were discussed in relation to the various structural features of the alloys. The structure of the strongest Zn-0.8Mg alloy was composed of a fine mixture of α -Zn dendrites and α -Zn + Mg₂Zn₁₁ eutectics. The cytotoxicity was evaluated with an indirect contact assay using human osteosarcoma cells (U-2 OS). The cytotoxicity of the Zn-0.8Mg alloy extract was low and only slightly higher than in the case of the pure-Mg extract.

Keywords: biodegradable material, zinc, mechanical properties, structure, cytotoxicity

V tem delu so bile preučevane struktura, natezne, tlačne in upogibne mehanske lastnosti biorazgradljive zlitine Zn-Mg z masnim deležem od 0 % do 8,3 % Mg. Ugotovljeno je bilo, da sta bili pri zlitini Zn-0,8Mg doseženi največja natezna in tlačna trdnost 170 MPa oziroma 320 MPa. Ta zlitina je tudi pokazala največji raztezek 2 % pri natezni obremenitvi. Mehanske lastnosti so prikazane v odvisnosti od mikrostrukturnih značilnosti zlitin. Mikrostruktura najmočnejše zlitine Zn-0,8Mg je bila sestavljena iz α -Zn-dendritov in α -Zn + Mg₂Zn₁₁-evtektika. Citotoksičnost je bila ocenjena s posrednim preizkusom kontakta s celicami človeškega osteosarkoma (U-2 OS). Citotoksičnost ekstrakta zlitine Zn-0,8Mg je bila majhna in samo malo večja v primerjavi z ekstraktom čistega Mg.

Ključne besede: biorazgradljiv material, cink, mehanske lastnosti, struktura, citotoksičnost

1 INTRODUCTION

Biodegradable implant materials progressively degrade in the human body after the implantation, producing relatively non-toxic compounds and, simultaneously, they are being replaced by the growing tissue. Biodegradable polymeric materials have been known and used for a long time. However, polymeric materials are not suitable for the load-bearing applications such as screws or plates for fractured bones, due to their low mechanical strength.¹ Among biodegradable metallic materials, magnesium alloys have attracted the greatest interest since the beginning of the 20th century.² The reason for this is that magnesium is relatively non-toxic to the human body and excessive amounts of it can be readily excreted by the kidneys. Moreover, it is very important for many biological functions of the human body. The main disadvantage of most magnesium alloys explored so far is that they corrode too rapidly in physiological environments, producing excessive amounts of hydrogen and increasing the alkalinity close to the implant.²⁻⁶ Both factors retard the healing process. Therefore, large efforts have been devoted to finding magnesium-based alloys degrading at acceptably low rates and many kinds

of Mg-based alloys, like AZ, AM, LAE, WE, Mg-Zn, Mg-Zn-Ca, Mg-Zn-Mn-Ca, Mg-Zn-Y, Mg-Gd, Mg-Zn-Si and others, have been studied until now.⁷⁻¹⁶

In Mg-based biodegradable alloys, zinc is often one of the major constituents. Zinc is known to improve the strength and corrosion resistance of magnesium and, from the biological point of view, it is generally considered relatively non-toxic.¹⁷ In the majority of the Mg biodegradable alloys given above, the concentrations of zinc do not exceed several mass fractions *w*%. But a deep eutectic in the Mg-Zn binary-phase diagram¹⁸ with about 51 % Zn supports the glass-forming ability (GFA) of Mg-Zn-based alloys with high concentrations of zinc. Amorphous ternary Mg-Zn-Ca alloys whose compositions are close to the eutectic point were already prepared^{19,20} and shown to be promising candidates for biodegradable implants. Due to the unordered atomic structures and high Zn contents, amorphous alloys have an excellent strength, high corrosion resistance, low hydrogen evolution rate and a good biocompatibility in animals. Until now, bulk amorphous Mg-Zn-Ca samples of only a few millimeters in size have been prepared.

The fact that zinc is a biologically tolerable element, even when its content in Mg-based alloys approaches

$w = 50 \%$,²¹ indicates that Zn-based alloys may also be promising candidates for biodegradable implants. This has motivated our research of Zn-based biodegradable alloys. The main advantage of these materials over Mg-Zn metallic glasses is that they are much easier to prepare using the classical routes like gravity or die casting, hot rolling, hot extrusion, ECAP, etc. In our previous work²² we provided information on the basic mechanical and corrosion properties of three binary Zn-Mg alloys containing $w(\text{Mg}) = 1\text{--}3 \%$. We have shown that these alloys are significantly more corrosion resistant in a simulated body fluid (SBF) than Mg alloys. Possible zinc doses and toxicity were estimated and found to be negligible when compared to the tolerable biological daily limit of zinc. Magnesium was shown to strengthen the alloys and it is also known to support the healing process of the hard tissue.²²

To properly design a load-bearing implant, the mechanical properties of an implant material are of a great importance. For this reason, this work is focused on the mechanical characterization including the hardness, tensile, compressive and bending properties of a series of the Zn-Mg binary alloys containing $w(\text{Mg}) = 0\text{--}8 \%$. These limits were selected to be around the eutectic point in the Zn-Mg system (approximately $w(\text{Mg}) = 3 \%$).¹⁸ Moreover, the cytotoxicity of zinc was also assessed and compared with magnesium and other elements.

2 EXPERIMENTAL WORK

In this study, pure zinc and six binary Zn-Mg alloys containing $w = 0.8\text{--}8.3 \%$ of Mg were studied. The designations and chemical compositions of the studied alloys are given in **Table 1**.

Zn-based alloys were prepared by melting pure zinc (99.95 %) and magnesium (99.90 %) in a resistance furnace in air. To prevent an excessive evaporation of volatile zinc, the melting temperature did not exceed 500 °C, and the homogenization was ensured with an intense mechanical stirring using a graphite rod. After a sufficient homogenization, the melts were poured into a cast-iron mold to prepare cylindrical ingots of 20 mm in diameter and 130 mm in length. The chemical compositions were verified at both ends of the ingots with X-ray fluorescence spectrometry (XRF), as shown in **Table 1**.

The structures of the alloys were studied using light (LM) and scanning electron microscopy (SEM, Tescan Vega 3) with energy dispersive X-ray spectrometry (EDS, Oxford Instruments Inca 350). The phase composition

was also confirmed with an X-ray diffraction analysis (XRD, X Pert Pro).

The mechanical properties of the as-cast alloys were characterized with hardness, tensile, compressive and bending tests. The samples for these tests were cut directly from the as-cast ingots. A loading of 5 kg was used for Vickers-hardness measurements. The rod samples for tensile tests had a diameter and length of 10 mm and 120 mm, respectively. Compressive tests were realized with rectangular samples of 10 mm × 10 mm × 15 mm in size. The compressive loading direction was parallel to the longest dimension. For three-point bending tests, rod samples of 4 mm in diameter and 40 mm in length were used. All the mechanical tests used a deformation rate of 1 mm/min. Fracture surfaces were examined after the tensile and bending tests using SEM.

The cytotoxicity of Zn-Mg alloys was assessed by using human osteosarcoma cells (U-2 OS). The investigated Zn-0.8Mg alloy and pure magnesium were used in these tests. Pure magnesium was used for comparison because it is generally considered to have a good biocompatibility and it is, thus, the basis of the most extensively studied metallic biomaterials. Before the extraction, cells were cultured in Dulbecco's modified Eagle's medium (DMEM) with a 10 % fetal bovine serum (FBS), 100 U/mL penicillin, 1 mg/mL streptomycin and 250 ng/mL amphotericin B at 37 °C in a humidified atmosphere of 5 % CO₂. The cytotoxicity was evaluated with an indirect-contact assay. Extracts were prepared by immersing the alloys in a DMEM medium containing a 5 % FBS and antibiotics at 37 °C for 7 d. The ratio of the surface area of the alloy samples to the extraction medium was 1 cm²/mL. The extracts were then withdrawn and diluted twice. The concentrations of Zn and Mg released from Zn-0.8Mg and Mg, respectively, were determined using inductively coupled plasma mass spectrometry (ICP MS). The cells were seeded at a density of cells $2.5 \times 10^4 \text{ mL}^{-1}$ and incubated in 96-well cell culture plates for 24 h to allow attachment. The medium was then replaced with 100 µL of the extracts. The controls for a comparison of the cell viability involved both pure DMEM medium (100 % viability) and 0.64 % phenol in the DMEM medium as the toxic control. After the incubation of the cells in a humidified atmosphere of 5 % CO₂ at 37 °C for 1 d the extracts were removed. The cells were then washed twice using phosphate buffered saline (PBS) and overlaid with a phenol red-free DMEM medium containing 5 µL of the WST-1 reagent (Roche) per well. The plates were incubated with WST-1 for 4 h at 37 °C. The assay is based on the reduction of tetrazolium salt to soluble formazan due to mitochondrial enzymes of the viable

Table 1: Chemical compositions of the investigated alloys in mass fractions ($w/\%$)

Tabella 1: Kemijske sestave preiskovanih zlitin v masnih deležih ($w/\%$)

Alloy designation	Zn	Zn-0.8Mg	Zn-1.6Mg	Zn-2.5Mg	Zn-3.5Mg	Zn-5.4Mg	Zn-8.3Mg
Mg concentration	<0.01	0.79 ± 0.05	1.57 ± 0.04	2.51 ± 0.03	3.47 ± 0.03	5.36 ± 0.12	8.32 ± 0.04

cells. The absorbance of the samples characterizing the cell viability was measured using a microplate reader at 450 nm with a reference wavelength of 630 nm. The higher the absorbance, the higher is the viability of the cells.

3 RESULTS AND DISCUSSION

3.1 Structures

The light micrographs of the investigated alloys are shown in **Figure 1**. It is seen in **Figure 1a** that the pure zinc is composed of almost equi-axed grains of approximately 20 μm in size. The structures of the alloys from Zn-0.8Mg to Zn-2.5Mg (**Figures 1b to 1d**) are hypoeutectic, i.e., they are composed of the primary α -Zn dendrites (light) and the α -Zn + $\text{Mg}_2\text{Zn}_{11}$ eutectic mixture (dark) in interdendritic regions, dominated by the lamellar and rod morphologies of the eutectic phases (see also a detailed view inserted in **Figure 1d**). The presence of the two phases of α -Zn and $\text{Mg}_2\text{Zn}_{11}$ in the alloys was also confirmed with XRD (not shown). The

average thickness of the dendritic branches in these alloys is approximately 30 μm and the volume fraction of the eutectic mixture increases with the increasing Mg concentration. In all the hypoeutectic alloys the average eutectic interparticle spacing is approximately 2 μm (**Figure 1d**). The composition of the Zn-3.5Mg alloy is very close to the eutectic point in the binary Zn-Mg phase diagram.¹⁸ Its structure (**Figure 1e**) is, thus, dominated by a very fine rod-and-lamellar α -Zn + $\text{Mg}_2\text{Zn}_{11}$ eutectic mixture, in which the average eutectic interparticle spacing is close to that in the previous alloys (2 μm). The eutectic mixture creates the colonies of 50–200 μm in size that differ in the spatial orientation of the rods and lamellae. The Zn-5.4Mg and Zn-8.3Mg alloys (**Figures 1f and 1g**, respectively) are hypereutectic, containing sharp-edged $\text{Mg}_2\text{Zn}_{11}$ intermetallic phases (light) and the α -Zn+ $\text{Mg}_2\text{Zn}_{11}$ eutectic mixture (dark). Rod and lamellar eutectic particles are observed (**Figure 1g**). Like in the hypoeutectic and eutectic alloys, the average eutectic interparticle spacing is approximately 2 μm . The volume fraction and dimensions of the primary inter-

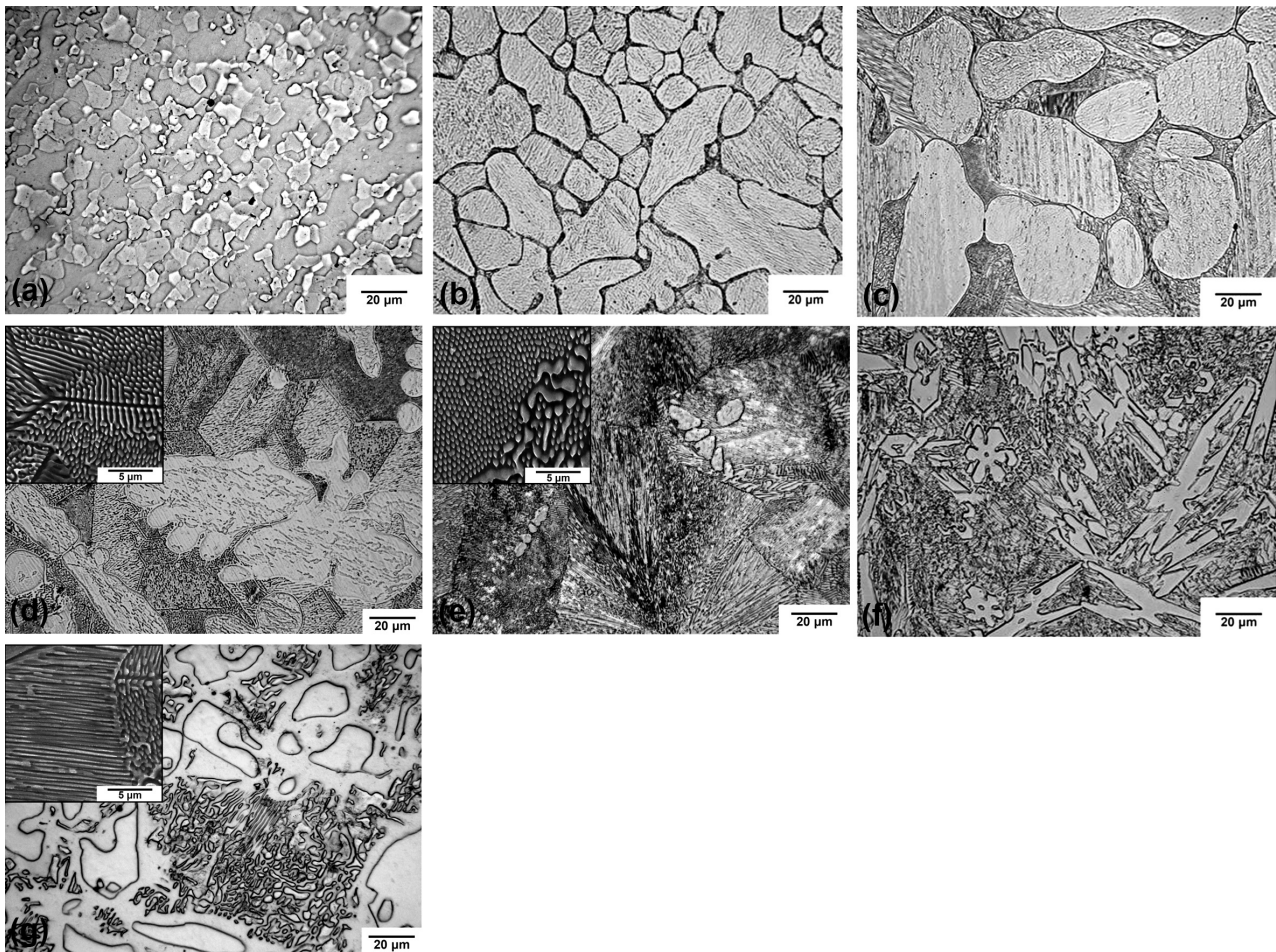


Figure 1: Light and detailed SEM micrographs of the alloys: a) Zn, b) Zn-0.8Mg, c) Zn-1.6Mg, d) Zn-2.5Mg, e) Zn-3.5Mg, f) Zn-5.4Mg, g) Zn-8.3Mg

Slika 1: Svetlobni in podrobni SEM-posnetki mikrostrukture zlitin: a) Zn, b) Zn-0,8Mg, c) Zn-1,6Mg, d) Zn-2,5Mg, e) Zn-3,5Mg, f) Zn-5,4Mg, g) Zn-8,3Mg

metallic phases increase with the increasing Mg contents in the alloys. The nature of the Mg_2Zn_{11} intermetallic phases was verified with XRD (not shown) and EDS, determining mole fractions $x = 15.1\%$ Mg and $x = 84.9\%$ Zn in these particles. Due to enrichment in magnesium, the particles are often surrounded by a thin layer of the α -Zn phase.

3.2 Mechanical properties

Figure 2 shows various mechanical properties of the Zn-Mg alloys as functions of the Mg content. One can see that there is a direct relationship between the Mg content and mechanical properties. The hardness of the Zn-Mg alloys increases with the Mg concentration from approximately 37 HV5 for the pure zinc up to 226 HV5 for the Zn-8.3Mg alloy (**Figure 2a**). This behavior can be attributed to the increasing volume fraction of the hard Mg_2Zn_{11} intermetallic phase due to magnesium (**Figure 1**).

The compressive mechanical properties summarized in **Figure 2b** show a similar trend, i.e., the compressive yield strength increases with the Mg concentration from 80 MPa (the pure zinc) up to 625 MPa (the Zn-3.5Mg alloy). The ultimate compressive strength of the alloys containing 0–3.5 % Mg was not measured because they were not broken during the loading, suggesting a good compressive plasticity of hypoeutectic and eutectic alloys. In the case of hypoeutectic alloys this plasticity is attributable to a relatively large volume fraction of the soft α -Zn phase (**Figures 1a to 1d**). The compressive plasticity of the eutectic Zn-3.5Mg alloy is a little surprising because this alloy contains approximately volume fraction $\varphi = 50\%$ of the brittle Mg_2Zn_{11} eutectic phase (**Figure 1e**). A detailed insert in **Figure 1e** shows that the eutectic mixture is very fine and that the average diameter of eutectic rods and the thickness of eutectic lamellae do not significantly exceed 1 μm . During the compressive loading, hard eutectic particles act as stress concentrators. The larger are the particles, the higher is the local-stress increase around them. In the case of fine eutectic particles, the local-stress increase in their vicinity is probably small; therefore, the alloy shows an unlimited plastic deformation in compression. In contrast, at higher Mg concentrations the fracture took place before the onset of the plastic deformation, therefore, only the values of the ultimate compressive strength of the Zn-5.4Mg and Zn-8.3Mg alloys are shown in **Figure 2b**. Both these alloys contain sharp-edged primary Mg_2Zn_{11} intermetallic phases (**Figures 1f to 1g**). Their sizes, shapes and brittle nature indicate that the stress concentration around them is high. Fracture cracks, thus, grow at a low nominal compressive stress of slightly above 200 MPa, i.e., significantly below the onset of the plastic deformation.

Bending mechanical properties are illustrated in **Figure 2c**. It is observed that a bending strength first

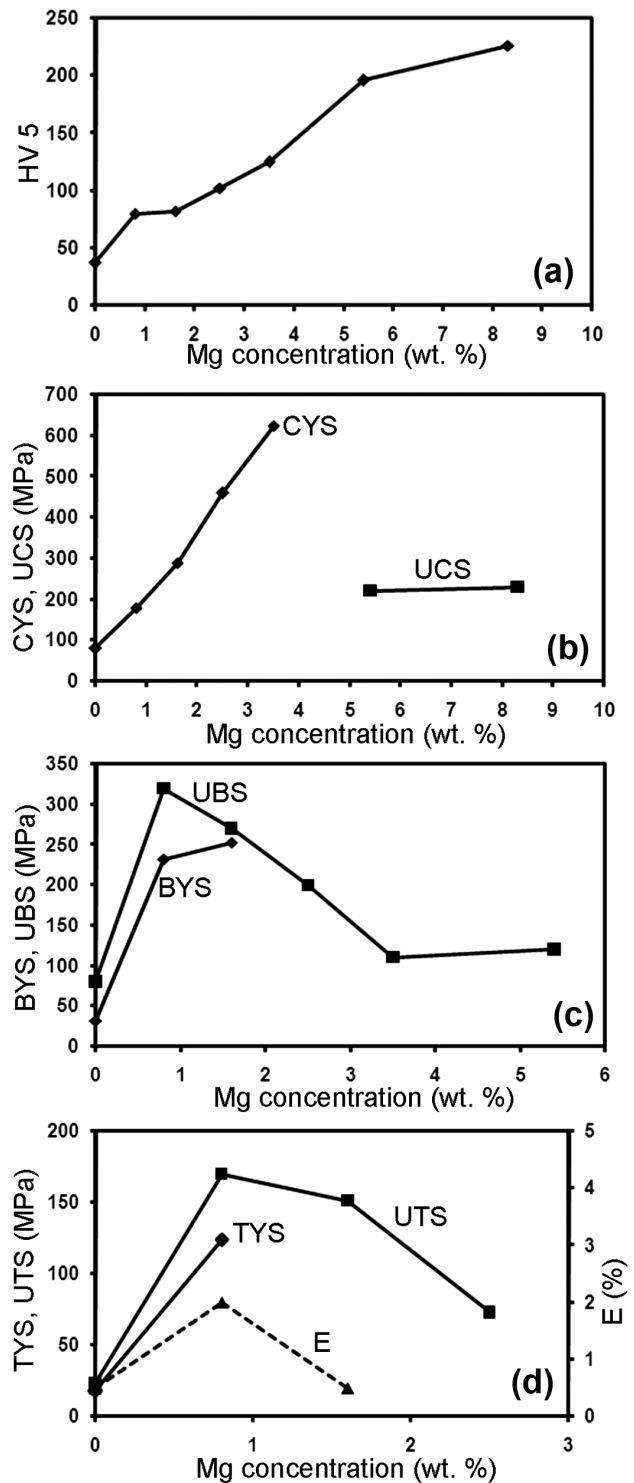


Figure 2: Mechanical properties of Zn-Mg alloys versus Mg concentration: a) Vickers hardness HV5, b) compressive tests (UCS – ultimate compressive strength, CYS – compressive yield strength), c) bending tests (UBS – ultimate bending strength, BYS – bending yield strength), d) tensile tests (UTS – ultimate tensile strength, TYS – tensile yield strength, E – elongation)

Slika 2: Mehanske lastnosti zlitin Zn-Mg glede na koncentracijo Mg: a) trdota po Vickersu HV5, b) tlačni preizkus (UCS – končna tlačna trdnost, CYS – meja plastičnosti pri tlačnem preizkusu), c) upogibni preizkus (UBS – končna upogibna trdnost, BYS – meja plastičnosti pri upogibnem preizkusu), d) natezni preizkus (UTS – končna natezna trdnost, TYS – meja plastičnosti pri nateznem preizkusu, E – raztezek)

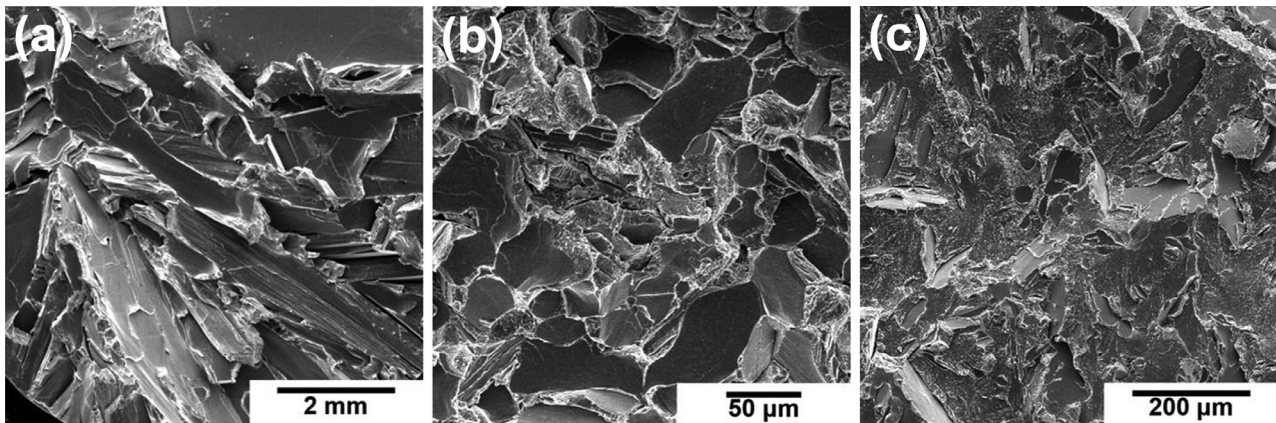


Figure 3: Fracture surfaces of Zn-Mg alloys after the tensile tests: a) Zn, b) Zn-0.8Mg, c) Zn-2.5Mg
Slika 3: Površina preloma zlitin Zn-Mg po nateznih preizkusih: a) Zn, b) Zn-0,8Mg, c) Zn-2,5 Mg

increases with the increasing Mg concentration and reaches the maximum of 320 MPa at 0.8 % Mg. At higher Mg concentrations, the bending strength progressively reduces to 110–120 MPa at 3.5–5.4 % Mg. The bending yield strength also increases with the increasing Mg concentration, i.e., with the increasing volume fraction of the eutectic mixture, and reaches 253 MPa at 1.6 % Mg. The alloys with higher Mg amounts fracture before the onset of the macroscopic plastic deformation. The results illustrated in **Figure 2c** also show that the plasticity of Zn-Mg alloys during bending is lower compared to that during compressive loading. In the compressive tests, the Zn-3.5Mg alloy can withstand a significant plastic deformation, whereas in the bending tests this alloy is macroscopically brittle. The reason for this difference is in the nature of the local stresses in the alloys during loading. During macroscopic compressive loading, the compressive component of the local stresses predominates. On the other hand, bending induces the local tensile stresses supporting the formation and growth of defects and macroscopic fracture cracks.

Tensile mechanical properties are summarized in **Figure 2d**. As in the previous case, the ultimate tensile strength increases up to 170 MPa at 0.8 % Mg. Higher Mg concentrations lead to a decrease in the ultimate tensile strength to 73 MPa for the Zn-2.5Mg alloy. The tensile yield strength reaches the maximum of 124 MPa at 0.8 % Mg. At this concentration an elongation of the alloy is 2 %. The alloys with the Mg concentrations above this limit fractured before the macroscopic plastic deformation due to an increased fraction of the brittle Mg_2Zn_{11} phase. These results confirm the above finding that the plasticity of Zn-Mg alloys decreases with the increasing tensile component during loading. In the tensile testing, the most detrimental tensile-stress component is the most pronounced supporting an easy nucleation and growth of fracture cracks.

The fracture surfaces of the selected alloys after tensile testing are shown in **Figure 3**. One can observe that zinc shows a brittle and intercrystalline fracture

(**Figure 3a**) without any plastic deformation. Individual grains are clearly visible in this figure. **Figure 3b** shows the fracture surface of the Zn-0.8Mg alloy with the highest bending and tensile strengths. In contrast to the pure zinc, this surface has a significantly refined morphology, in which both the primary zinc and eutectic (**Figure 1b**) can be clearly distinguished. The primary zinc dendrites are characterized by an almost brittle fracture that corresponds to the flat facets on the fracture surface. The eutectic mixture that surrounds these facets exhibits a refined morphology and there is an indication of a plastic deformation in this area. The refined fracture morphology with a certain degree of plastic deformation is associated with improved bending and tensile strengths of this alloy because both the fine grains and the hard network represent barriers for the growing crack. It appears that the Zn-0.8Mg alloy provides the optimum volume fractions of both structural components. The fracture surface of the Zn-2.5Mg alloy in **Figure 3c** also includes the flat facets of the primary α -Zn and the regions of refined morphology corresponding to the α -Zn + Mg_2Zn_{11} eutectic mixture (**Figure 1d**). But a high portion of the brittle Mg_2Zn_{11} eutectic phase negatively affects both the bending and tensile strengths because this phase acts as a source of defects during mechanical loading at which fracture cracks nucleate.

Based on the results shown in **Figure 2**, it can be assumed that the Zn-0.8Mg alloy is the most promising material for load-bearing implants because it reaches the maximum bending and tensile strengths of 320 MPa and 168 MPa, respectively. The Zn-0.8Mg alloy also shows a good plasticity in all three loading modes. In compression this alloy is able to be deformed without a fracture. When considering an application of Zn-Mg alloys as, for example, the fixation screws or plates for fractured bones, the mechanical properties of the alloys should be compared to those of bones or other biomaterials. **Table 2** provides a summary of the tensile, compressive and bending mechanical properties of bones, the Zn-0.8Mg

Table 2: Basic mechanical properties of various biomaterials and natural bones (PLA-poly(lactic acid))^{1,23-28}
Tabela 2: Osnovne mehanske lastnosti različnih biomaterialov in naravnih kosti (PLA-polimlečna kislina)^{1,23-28}

Tissue/material	Density (g/cm ³)	Tensile strength (MPa)	Elastic modulus (GPa)	Compressive strength (MPa)	Bending strength (MPa)
Bone	≈ 2	30–280	5–20	160–240	2–150
Zn-0.8Mg	≈ 7	170	≈ 90	–	320
PLA	≈ 1	≈ 50	≈ 3	–	60–150
Hydroxyapatite	≈ 3	10–80	70–100	60–500	≈ 50
Wrought Ti-based alloy	≈ 4.5	700–1200	110	–	–
Wrought Co-based alloy	≈ 8.5	600–1000	220	–	–
Wrought stainless steels	≈ 8	800–1100	200	–	–

alloy, biodegradable polymers (poly(lactic acid), PLA), hydroxyapatite, inert Ti-, Co- and Fe-based alloys.^{1,23-28} One can see that the Zn-0.8Mg alloy is characterized by significantly higher tensile and bending strengths as compared to the biodegradable PLA and hydroxyapatite. Moreover, the strength and elastic modulus of this alloy are much closer to those of the bone, as compared to the inert Ti-, Co- or Fe-based biomaterials.

3.3 Cytotoxicity

The Zn and Mg concentrations in the extracts prepared using the Zn-0.8Mg alloy and Mg are 4 µg/mL and 43 µg/mL, respectively. The significantly lower concentration of zinc results from a much better corrosion resistance of the zinc alloy as compared to magnesium, as shown in our previous work.²² **Figure 4** illustrates the cytotoxic effects of the extracts on the U-2 OS cells, expressed as the percent absorbance of the DMEM control. It is observed that pure magnesium is tolerated well by U-2 OS cells because these cells are fully viable in the extract containing 43 µg/mL Mg (almost a 100 % absorbance). This measurement confirms the presumption stated in the experimental section that magnesium has a good biocompatibility. What is more important in this study is that the U-2 OS cells exposed to the extract from the Zn-0.8Mg alloy also show a good viability of 80 %, i.e., only slightly lower than in the case of the Mg

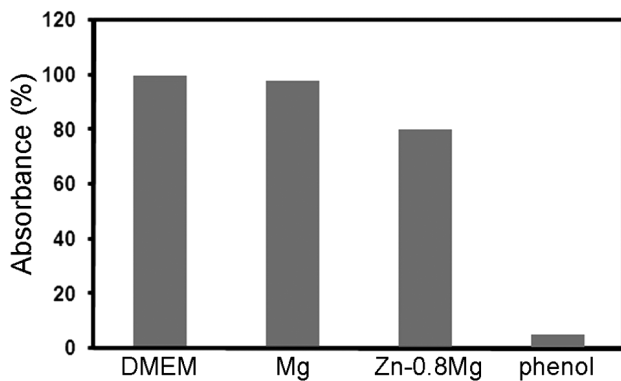


Figure 4: Cytotoxic effects of diluted extracts on the U-2 OS cells, expressed as the percent absorbance of the DMEM control

Slika 4: Citotoksičen vpliv raztopljenih ekstraktov na celice U-2 OS, izražen kot delež absorbance kontrolnega DMEM

extract. Due to a low corrosion rate of zinc,²² its concentrations in the extracts are very low and, therefore, such extracts are not toxic for the cells. A similar situation can be expected in the case of Zn implants in the human body. The zinc present in the body fluids would probably not cause any toxic effects, despite the lower tolerable biological limits of zinc as compared to magnesium.

4 CONCLUSIONS

Biodegradable Zn-Mg alloys containing from 0 % to more than 8 % Mg were investigated in this work. It was shown that only the alloys containing relatively low concentrations of Mg (approximately 1 %) are suitable for the load-bearing implants in the as-cast state, because they have high tensile and bending strengths and an acceptable elongation. The strength of such alloys is higher than those of biodegradable polymers and hydroxyapatite and comparable to that of the bones. Good mechanical properties result from a relatively fine structure composed of primary zinc and interdendritic eutectic. It is assumed that an additional improvement in the strength can be achieved with hot extrusion. At the Mg concentrations of above 1 %, Zn-Mg alloys become relatively brittle mainly during tensile loading.

Zn-Mg alloys can be considered as the alternatives to Mg-based biodegradable alloys. The main advantage of zinc alloys over magnesium alloys lies in their significantly better corrosion resistance in simulated body fluids. Therefore, the concentrations of the Zn ions extracted from alloys are low and they do not cause any significant toxic effects, as demonstrated with the cytotoxicity tests involving human osteosarcoma U-2 OS cells in this study.

Acknowledgements

The research of the biodegradable metallic materials was financially supported by the Czech Science Foundation (project no. P108/12/G043).

5 REFERENCES

¹ J. R. Davis, Handbook of materials for medical devices, ASM International, Materials Park 2003

- ² F. Witte, The history of biodegradable magnesium implants: a review, *Acta Biomater*, 6 (2010), 1680–92
- ³ C. Y. Zhang, R. C. Zeng, C. L. Liu, J. C. Gao, Comparison of calcium phosphate coatings on Mg-Al and Mg-Ca alloys and their corrosion behavior in Hank's solution, *Surface and Coatings Technology*, 204 (2010), 3636–40
- ⁴ M. D. Pereda, C. Alonso, L. Burgos-Asperilla, J. A. del Valle, O. A. Ruano, P. Perez et al., Corrosion inhibition of powder metallurgy Mg by fluoride treatments, *Acta Biomater*, 6 (2010), 1772–82
- ⁵ J. E. Gray-Munro, C. Seguin, M. Strong, Influence of surface modification on the in vitro corrosion rate of magnesium alloy AZ31, *J Biomed Mater Res A*, 91 (2009), 221–30
- ⁶ S. Hiromoto, T. Shishido, A. Yamamoto, N. Maruyama, H. Somekawa, T. Mukai, Precipitation control of calcium phosphate on pure magnesium by anodization, *Corrosion Science*, 50 (2008), 2906–13
- ⁷ R. Erbel, C. Di Mario, J. Bartunek, J. Bonnier, B. de Bruyne, F. R. Eberli et al., Temporary scaffolding of coronary arteries with bioabsorbable magnesium stents: a prospective, non-randomised multi-centre trial, *Lancet*, 369 (2007), 1869–75
- ⁸ C. Di Mario, H. Griffiths, O. Goktekin, N. Peeters, J. Verbist, M. Bosiers et al., Drug-eluting bioabsorbable magnesium stent, *J Interv Cardiol*, 17 (2004), 391–5
- ⁹ P. Peeters, M. Bosiers, J. Verbist, K. Deloosse, B. Heublein, Preliminary results after application of absorbable metal stents in patients with critical limb ischemia, *Journal of endovascular therapy: an official journal of the International Society of Endovascular Specialists*, 12 (2005), 1–5
- ¹⁰ S. Zhang, X. Zhang, C. Zhao, J. Li, Y. Song, C. Xie et al., Research on an Mg-Zn alloy as a degradable biomaterial, *Acta Biomater*, 6 (2010), 626–40
- ¹¹ Z. Li, X. Gu, S. Lou, Y. Zheng, The development of binary Mg-Ca alloys for use as biodegradable materials within bone, *Biomaterials*, 29 (2008), 1329–44
- ¹² E. Zhang, L. Yang, J. Xu, H. Chen, Microstructure, mechanical properties and bio-corrosion properties of Mg-Si(-Ca, Zn) alloy for biomedical application, *Acta Biomater*, 6 (2010), 1756–62
- ¹³ E. Zhang, L. Yang, Microstructure, mechanical properties and bio-corrosion properties of Mg-Zn-Mn-Ca alloy for biomedical application, *Materials Science and Engineering A*, 497 (2008), 111–8
- ¹⁴ X. N. Gu, W. Zheng, Y. Cheng, Y. F. Zheng, A study on alkaline heat treated Mg-Ca alloy for the control of the biocorrosion rate, *Acta Biomater*, 5 (2009), 2790–9
- ¹⁵ Z. G. Huan, M. A. Leeflang, J. Zhou, L. E. Fratila-Apachitei, J. Duszczuk, In vitro degradation behavior and cytocompatibility of Mg-Zn-Zr alloys, *Journal of materials science, Materials in medicine*, 21 (2010), 2623–35
- ¹⁶ F. Witte, N. Hort, C. Vogt, S. Cohen, K. U. Kainer, R. Willumeit et al., Degradable biomaterials based on magnesium corrosion, *Current Opinion in Solid State and Materials Science*, 12 (2008), 63–72
- ¹⁷ G. J. Fosmire, Zinc toxicity, *Am J Clin Nutr*, 51 (1990), 225–7
- ¹⁸ W. F. Gale, T. C. Totemeier, *Smithells Metals Reference Book*, 8th Edition, Elsevier Publishers, 2004
- ¹⁹ X. Gu, Y. Zheng, S. Zhong, T. Xi, J. Wang, W. Wang, Corrosion of, and cellular responses to Mg-Zn-Ca bulk metallic glasses, *Biomaterials*, 31 (2010), 1093–103
- ²⁰ Q. F. Li, H. R. Weng, Z. Y. Suo, Y. L. Ren, X. G. Yuan, K. Q. Qiu, Microstructure and mechanical properties of bulk Mg-Zn-Ca amorphous alloys and amorphous matrix composites, *Materials Science and Engineering A*, 487 (2008), 301–8
- ²¹ B. Zberg, P. J. Uggowitzer, J. F. Löffler, MgZnCa glasses without clinically observable hydrogen evolution for biodegradable implants, *Nat Mater*, 8 (2009), 887–91
- ²² D. Vojtech, J. Kubasek, J. Serak, P. Novak, Mechanical and corrosion properties of newly developed biodegradable Zn-based alloys for bone fixation, *Acta Biomater*, 7 (2011), 3515–22
- ²³ J. R. Davis (ed.), *ASM Handbook: Volume 2, Properties and Selection: Nonferrous Alloys and Special-Purpose Materials*, Handbook A, ASM International, Materials Park 1990
- ²⁴ G. E. J. Poinern, S. Brundavanam, D. Fawcett, Biomedical Magnesium Alloys: A Review of Material Properties, Surface Modifications and Potential as a Biodegradable Orthopaedic Implant, *American Journal of Biomedical Engineering*, 2 (2013), 218–40
- ²⁵ D. K. Pattanayak, P. Divya, S. Upadhyay, R. C. Prasad, B. T. Rao, T. R. Rama Mohan, Synthesis and Evaluation of Hydroxyapatite Ceramics, *Trends Biomater Artif Organs*, 18 (2005), 87–92
- ²⁶ N. Monmaturapoj, C. Yatongcha, Effect of Sintering on Microstructure and Properties of Hydroxyapatite Produced by Different Synthesizing Methods, *Journal of Metals, Materials and Minerals*, 20 (2010), 53–61
- ²⁷ S. Pramanik, A. K. Agarwal, K. N. Rai, Development of High Strength Hydroxyapatite for Hard Tissue Replacement, *Trends Biomater Artif Organs*, 19 (2005), 46–51
- ²⁸ A. J. Ruys, M. Wei, C. C. Sorrell, M. R. Dickson, A. Brandwood, B. K. Milthorpe, Sintering effects on the strength of hydroxyapatite, *Biomaterials*, 16 (1995), 409–15